

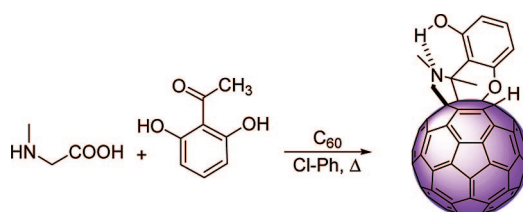
H-Bond-Assisted Regioselective (*cis-1*) Intramolecular Nucleophilic Addition of the Hydroxyl Group to [60]Fullerene

Marta Izquierdo,[†] Sílvia Osuna,[‡] Salvatore Filippone,[†] Angel Martín-Domenech,[†] Miquel Solà,^{*,‡} and Nazario Martín^{*,†}

Departamento de Química Orgánica, Facultad de Química, Universidad Complutense, E-28040 Madrid, Spain, and Institut de Química Computacional and Departament de Química, Universidad de Girona, E-17071 Girona, Catalonia, Spain

nazmar@quim.ucm.es

Received September 26, 2008



The one-step reaction of 2,6-dihydroxyphenylmethyl ketone and sarcosine with [60]fullerene in refluxing chlorobenzene affords, in a totally regioselective process, the *cis-1* bicyclic-fused organofullerene through a new intramolecular nucleophilic addition of one hydroxy group to the fullerene double bond. Experimental findings reveal the presence of a methyl group on C-2 of the pyrrolidine ring as an essential requirement for the cyclization process, whereas the existence of a H-bond between a second hydroxylic group and the nitrogen atom of the pyrrolidine ring seems to favor the approaching geometry without determining the reaction outcome. Theoretical calculations using the two-layered ONIOM approach and density functional theory support the experimental findings, predicting the strong impact that the presence of the methyl substituent on the C-2 of the pyrrolidine ring has on the molecular geometry and, hence, on the intramolecular cyclization process.

Introduction

Since the preparation of fullerenes in macroscopic quantities in 1990,¹ a plethora of fullerene derivatives have been synthesized by following the wide variety of effective methods currently available for the chemical modification of fullerenes.² In this regard, despite the intensive efforts dedicated to the functionalization of fullerenes, a wide variety of fundamental reactions in the arsenal of organic chemistry have never been investigated in fullerene science.³ Furthermore, still there is a demand to develop better protocols to prepare tailor-made

fullerenes with desired specific chemical and electronic structures of interest in materials science and biomedical applications.⁴

Cycloaddition reactions, in particular, Diels–Alder and 1,3-dipolar cycloaddition, have been, by large, the most studied and successful reactions for preparing fullerene derivatives. However, nucleophilic addition of carbon nucleophiles as well as other species involving nitrogen (cyanide, amines), oxygen (alkoxides, hydroxides), phosphorus, and others such as silicon and germanium have also been extensively studied and a wide variety of derivatives bearing heteroatoms were prepared.²

We have recently developed a methodology directed to the synthesis of novel fused pyrrolidinofullerenes, from suitably functionalized pyrrolidino[3,4:1,2][60]fullerenes, as starting materials for preparing a variety of unprecedented modified fullerenes.⁵

[†] Universidad Complutense.

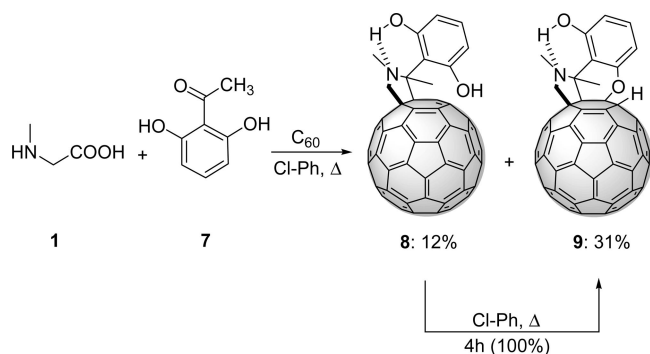
[‡] Universidad de Girona.

(1) Krätschmer, W.; Lamb, L. D.; Fostiropoulos, K.; Huffman, D. R. *Nature (London)* **1990**, *347*, 354–358.

(2) For some recent books, see: (a) Hirsch, A. *The Chemistry of Fullerenes*; Wiley-VCH: Weinheim, Germany, 2005. (b) *Fullerenes: From Synthesis to Optoelectronic Properties*; Guldi, D. M., Martín, N., Eds.; Kluwer Academic Publishers: Dordrecht, The Netherlands, 2002. (c) Taylor, R. *Lecture Notes on Fullerene Chemistry: A Handbook for Chemists*; Imperial College Press: London, 1999. (d) *Fullerenes*; Langa, F., Nierengarten, J.-F., Eds.; RSC Publishing: Cambridge, U.K., 2007.

(3) Martín, N.; Altable, M.; Filippone, S.; Martín-Domenech, A. *Synlett* **2007**, *20*, 3077–3095.

(4) (a) Nierengarten, J.-F. *Top. Curr. Chem.* **2003**, *228*, 87. (b) Nierengarten, J.-F. *New J. Chem.* **2004**, *28*, 1177–1191. (c) Martín, N. *Chem. Commun.* **2006**, 2093–2104.

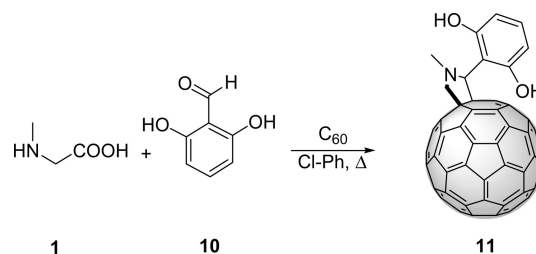
SCHEME 3. 1,3-Dipolar Cycloaddition Reaction of Sarcosine and 2,6-Dihydroxyphenyl Methyl Ketone


To favor the chemical reactivity of these fullerenes, a double substitution should be present on C-2 of the pyrrolidine ring, similarly to the Thorpe–Ingold effect previously observed for fuller-1,6-enynes.⁵ In this regard, fulleropyrrolidines bearing a methyl group on the C-2 of the pyrrolidine ring fulfill the above requirements, resulting in a different geometry for the reaction of the OH with the fullerene double bond, and in addition, they were easily prepared in one simple synthetic step. Thus, we have obtained compound **6** in 25% yield (50% based on recovered C₆₀) by reaction of sarcosine (*N*-methylglycine, **1**), commercially available *o*-hydroxyphenyl methyl ketone (**5**), and C₆₀ in refluxing chlorobenzene. It is worth mentioning that the reactions of sarcosine with ketones proceeds with yields and efficiencies lower than those reported for aldehydes.¹⁵

Interestingly, in contrast to the previous examples **3a,b**, the ¹H NMR spectrum of compound **6** reveals the presence of the proton of the OH group at 13.13 ppm (deshielding effect of ~2 ppm in comparison with compound **3a**), which clearly suggests the existence of a strong H-bond between the OH and the N atom of the pyrrolidine ring. This experimental result indicates that the H-bond is formed with preference to the nucleophilic addition of the OH to the fullerene double bond, thus supporting the experimental findings for the location of the OH group atop the fullerene sphere.¹⁴ Once again, although two possible atropisomers can be obtained for **6**, only one was observed according to NMR data (see Supporting Information) in a diastereoselective mode. This is confirmed by the relative energies of the optimized structures for the different conformers of structure **6** depicted in Figure S21 in Supporting Information.

Taking advantage of the above experimental findings, we decided to carry out the synthesis of new pyrrolidinofullerenes endowed with a phenyl group on the C-2 of the pyrrolidine ring bearing two OH groups at C-2' and C-6' positions. Furthermore, in order to favor the geometrical approach of the second OH group to the fullerene double bond, it is anticipated that a methyl group should also be present at C-2 of the pyrrolidine ring.

Thus, we designed compound **8**, which fulfils the above requirements. Its preparation also involves one synthetic step as is depicted in Scheme 3. Reaction of sarcosine (**1**) and C₆₀ with commercially available 2,6-dihydroxyphenyl methyl ketone (**7**) in chlorobenzene at reflux temperature yielded the expected

SCHEME 4. 1,3-Dipolar Cycloaddition Reaction of Sarcosine and 2,6-Dihydroxybenzaldehyde


compound **8** in 12% yield (50% based on recovered C₆₀), together with the desired cyclic compound **9** resulting from the intramolecular nucleophilic addition of the OH to the fullerene double bond, which was obtained as the main reaction product (31% yield, 50% based on recovered C₆₀). It is interesting to note that because of the chain length between the reactive OH and C=C groups, the favored cyclization process according to Baldwin's rules¹⁶ (*6-exo-trig*) affords a hexagonal heterocyclic ring (dihdropyran) fused simultaneously to the pyrrolidine and benzene rings. This results in a single chemical structure in which the fullerene sphere is covalently connected to a system formed by three rings that are forming a fourth ring through the intramolecular H-bond.

To prove that cyclic compound **9** is formed from the open compound **8** by subsequent intramolecular nucleophilic addition of the OH group to the fullerene double bond, **8** was heated in refluxing chlorobenzene for 4 h and quantitative transformation into cyclic compound **9** was observed by HPLC. Interestingly, the proton of the OH group forming the hydrogen bond in compounds **8** and **9** appeared significantly deshielded at 13.92 and 13.23 ppm, respectively, thus confirming the existence of the H-bond. Furthermore, the second free OH group of compound **8** was observed at 4.85 ppm, as expected for the phenol moiety, whereas compound **9** exhibited the proton connected to the sp³ carbon of the fullerene sphere at 6.29 ppm, in good agreement with related systems.¹⁷

It is worth mentioning that the intramolecular addition of the OH group to the double bond of the fullerene proceeds in a totally regioselective and site-selective manner forming exclusively the *cis-1* isomer¹⁸ in which the oxygen atom is linked to the carbon adjacent to the pyrrolidine ring.

To determine the influence that the presence of the methyl group on the C-2 of the pyrrolidine ring has on the cyclization process, resulting from the nucleophilic attack of the OH group to the fullerene double bond, affording compound **9**, we decided to carry out the reaction of 2,6-dihydroxybenzaldehyde (**10**) with sarcosine (**1**) and C₆₀ in refluxing chlorobenzene (Scheme 4).¹⁹ The formed compound **11** has two hydroxyl groups as in **8** and **9** but is lacking the methyl group on C-2, which has been replaced by a H atom.

The new compound **11** was obtained in 20% yield (28% based on recovered C₆₀), and the ¹H NMR spectrum clearly revealed a singlet at 11.76 ppm, which indicates the presence of a (weak) H-bonding between the OH group and the pyrrolidine nitrogen

(15) Maggini, M.; Menna, E. In *Fullerenes: From Synthesis to Optoelectronic Properties*; Guldi, D. M., Martín, N., Eds.; Kluwer Academic Publishers: Dordrecht, 2002; Chapter 1, pp 1–50. See also: (a) Illescas, B.; Rife, J.; Ortuño, R. M.; Martín, N. *J. Org. Chem.* **2000**, *65*, 6246–6248. (b) Illescas, B.; Martín, N.; Poater, J.; Solà, M.; Aguado, G. P.; Ortuño, R. M. *J. Org. Chem.* **2005**, *70*, 6929–6932.

(16) Baldwin, J. E. *J. Chem. Soc., Chem. Commun.* **1976**, 734–736.

(17) Altable, M.; Filippone, S.; Martín-Domenech, A.; Güell, M.; Solà, M.; Martín, N. *Org. Lett.* **2006**, *8*, 5959–5962.

(18) For a systematic and simple site labelling system to indicate the relative positional relationships of addends in fullerene derivatives, see: Hirsch, A.; Lamparth, I.; Karfunkel, H. R. *Angew. Chem., Int. Ed.* **1994**, *33*, 437–438.

(19) We want to thank to one of the referees for this interesting suggestion, which has allowed a better understanding of this cyclization process.

atom, similarly to that found in **3b**. Furthermore, in agreement with this finding, the other OH group appears at 4.75 ppm, as that found for compound **8**. Interestingly, the singlet of the C–H proton of the pyrrolidine ring appears at 5.81 ppm. The above assignment was ascertained by adding D₂O to the NMR tube and observing the disappearance of the two signals at 11.76 and 4.75 ppm corresponding to the hydroxyl groups, without altering the proton at 5.81 ppm.²⁰

This result clearly confirms the presence of the methyl group on C-2 of the pyrrolidine ring as a necessary requirement for the cyclization process. However, the presence of the H-bond between the OH group ortho to the phenyl ring and the N atom is not so critical since compound **8** having the H-bond is formed and isolated. Nevertheless, the presence of the H-bond seems to favor the cyclization process provided that it orientates favorably the second OH group on the phenyl ring to the fullerene surface.

Electrochemistry. We have studied the electrochemical properties of the novel compounds (**6**, **8**, and **9**) by cyclic voltammetry (CV) in *o*-DCB/MeCN (4:1) as solvent at room temperature and by using tetrabutylammonium perchlorate as the supporting electrolyte. The characteristic shapes of the redox waves and their unequivocal position on the potential scale virtually fingerprint the individual electrochemical properties of the different redox systems. For this reason, CV has been labeled as an electrochemical spectroscopy.²¹ In our case, the saturation of one olefinic double bond in fulleropyrrolidines **6** and **8** should lead, in principle, to electrochemical behavior different from that shown by the related compound **9** in which two fullerene double bonds are saturated. This should raise the LUMO energy level, and therefore the reduction waves should be shifted toward more negative potentials, thus slightly reducing their accepting ability.²² Therefore, a voltamperometric study of these compounds should allow us to determine the electronic effect of the substitution pattern on the electrochemical properties of the compounds obtained and, simultaneously, to use CV as a useful characterization technique.

Thus, pyrrolidino[3,4:1,2[60]fullerene (**6**) presented three reversible reduction waves (−0.859, −1.259, −1.831 V) at values more negative than those of the parent C₆₀ (−0.747, −1.152, −1.627 V) (see Supporting Information). Interestingly, compounds **8** and **9** showed a similar behavior with the first two reversible reduction waves (**8**: −0.871, −1.260 V; **9**: −0.854, −1.246 V) corresponding to the formation of the radical-anion and dianion species of the C₆₀ moiety.

To illustrate the electrochemical behavior of these organofullerenes, the CVs of **8** and **9** are shown in Figure 1. Compounds **8** and **9** showed, in addition to the first two reversible reduction waves, the presence of an irreversible additional wave at 1.888 V (**8**) and 1.885 V (**9**). The irreversible character of this third reduction wave suggests the participation of the organic addend. In fact, compound **8** presents another wave at 1.760 V, whereas this wave is observed for **9** at 2.095 V.

(20) Whereas the signals corresponding to the fullerene moiety are easily observed at 527, 575, 1150–1190 and 1432–1462 cm^{−1} in the FTIR spectra, the signals over 3000 cm^{−1} do not clarify the existence of H-bonding. This experimental finding has also been observed in related systems where the phenolic hydroxylic group is forming a H bond with a close nitrogen atom (Lachaud, F.; Quaranta, A.; Pellegrin, P. D.; Charlot, M.-F.; Un, S.; Leibl, W.; Aukauloo, A. *Angew. Chem., Int. Ed.* **2005**, *44*, 1536–1540). Nevertheless, the presence or absence of H-bonding is unambiguously determined by ¹H NMR spectroscopy.

(21) Heinze, J. *Angew. Chem., Int. Ed.* **1984**, *23*, 831–847.

(22) Echegoyen, L.; Echegoyen, L. E. *Acc. Chem. Res.* **1998**, *31*, 593–60.

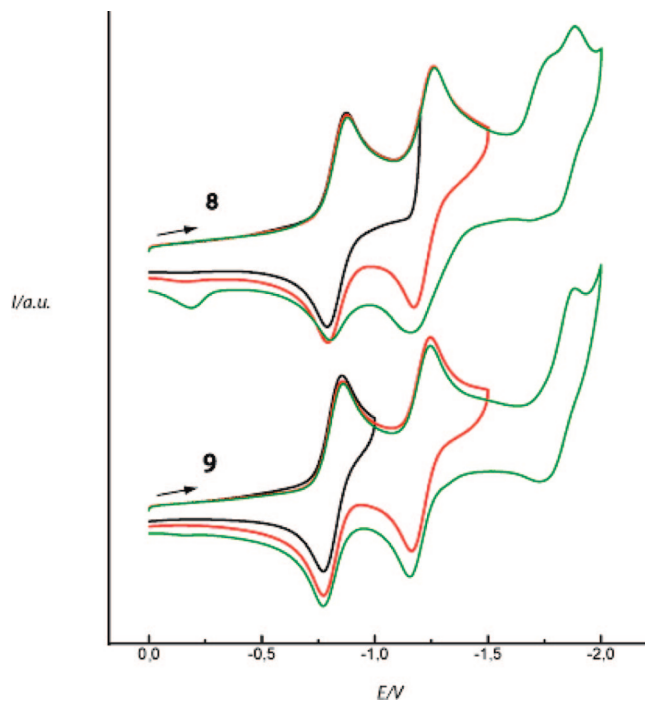


FIGURE 1. Cyclic voltammograms of compounds **8** and **9** measured in *o*-DCB/MeCN (4.1) at 100 mV s^{−1}.

Finally, although it could be expected that compound **9** exhibits a reduction wave significantly shifted to more negative values due to the saturation of two double bonds on the C₆₀ core, the experimental values reveal that the first reduction wave is very close to that found for the first reduction wave in compound **8** with only one saturated double bond. This finding can be accounted for by the presence of the electronegative oxygen atom directly connected to the fullerene skeleton, which decreases the LUMO energy, thus compensating the effect of the saturation of a second double bond in **9**.

This behavior is in agreement with other related examples in which the presence of strong electronegative atoms on the fullerene surface has a strong impact on the reduction potential values observed for these organofullerenes.²³

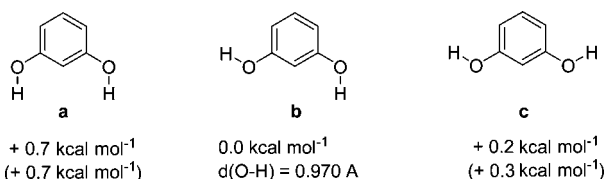
Computational Details. Full geometry optimizations were carried out with the two-layered ONIOM approach^{24,25} using the Gaussian 03 program.²⁶ The density functional theory (DFT) SVWN method^{27,28} together with the standard STO-3G basis set²⁹ was used for the low level calculations and the hybrid

(23) Suzuki, T.; Maruyama, Y.; Akasaka, T.; Ando, W.; Kobayashi, K.; Nagase, S. *J. Am. Chem. Soc.* **1994**, *116*, 1359–1363.

(24) Svensson, M.; Humbel, S.; Froese, R. D. J.; Matsubara, T.; Sieber, S.; Morokuma, K. *J. Phys. Chem.* **1996**, *100*, 19357–19363.

(25) Dapprich, S.; Komáromi, I.; Byu, K. S.; Morokuma, K.; Frisch, M. J. *J. Mol. Struct. (Theochem)* **1999**, *461–462*, 1–21.

(26) Frisch, M. J.; Trucks, G. W.; Schlegel, H. B.; Scuseria, G. E.; Robb, M. A.; Cheeseman, J. R.; Montgomery Jr., J. A.; Vreven, T.; Kudin, K. N.; Burant, J. C.; Millam, J. M.; Iyengar, S. S.; Tomasi, J.; Barone, V.; Mennucci, B.; Cossi, M.; Scalmani, G.; Rega, N.; Petersson, G. A.; Nakatsuji, H.; Hada, M.; Ehara, M.; Toyota, K.; Fukuda, R.; Hasegawa, J.; Ishida, M.; Nakajima, T.; Honda, Y.; Kitao, O.; Nakai, H.; Klene, M.; Li, X.; Knox, J. E.; Hratchian, H. P.; Cross, J. B.; Bakken, V.; Adamo, C.; Jaramillo, J.; Gomperts, R.; Stratmann, R. E.; Yazyev, O.; Austin, A. J.; Cammi, R.; Pomelli, C.; Ochterski, J. W.; Ayala, P. Y.; Morokuma, K.; Voth, G. A.; Salvador, P.; Dannenberg, J. J.; Zakrzewski, G.; Dapprich, S.; Daniels, A. D.; Strain, M. C.; Farkas, O.; Malick, D. K.; Rabuck, A. D.; Raghavachari, K.; Foresman, J. B.; Ortiz, J. V.; Cui, Q.; Baboul, A. G.; Clifford, S.; Cioslowski, J.; Stefanov, B. B.; Liu, G.; Liashenko, A.; Piskorz, P.; Komaromi, I.; Martin, R. L.; Fox, D. J.; Keith, T.; Al-Laham, M. A.; Peng, C. Y.; Nanayakkara, A.; Challacombe, M.; Gill, P. M. W.; Johnson, B.; Chen, W.; Wong, M. W.; Gonzalez, C.; Pople, J. A.; *Gaussian 03, Revision C.01*; Gaussian, Inc.: Pittsburgh, PA, 2003.

SCHEME 5. Different Conformers Considered for the Model System 1,3-Benzenediol^a


^a The relative energies represented in black have been calculated at the B3LYP/6-31G(d) level while energies in parentheses have been obtained using the MP2 method with 6-31G(d) basis set at the B3LYP/6-31G(d) optimized geometries.

density functional B3LYP method^{30–32} with the standard 6-31G(d) basis set^{33,34} was employed for the high level system. Single point calculations using the ab initio method MP2 at 6-31G(d) for the high level and the DFT method SVWN level with the STO-3G basis set for the low level (i.e., ONIOM2(MP2/6-31G(d):SVWN/STO-3G)//ONIOM2(B3LYP/6-31G(d):SVWN/STO-3G)) were performed. All systems were treated with the spin-restricted formalism. All transition states (TSs) were characterized by computing the analytical vibrational frequencies, to have one (*and only one*) imaginary frequency corresponding to the approach of the two reacting molecules. Calculations of the intrinsic reaction coordinate (IRC) to ensure that the TSs located in this work were connecting the expected reactants and products is extremely computationally demanding. Instead, a full optimization of each transition state was done by slightly shifting the geometry of the transition state in either sense following the direction of the transition vector (the eigenvector corresponding to the negative eigenvalue). Although this is not equivalent to performing an IRC, it gives a first idea of which reactants and products are connected through a given TS.

Theoretical Results and Discussion. Our analysis starts with the B3LYP/6-31G(d) study of the different conformers of the 1,3-benzenediol, where the hydroxyl groups can adopt different conformations (see Scheme 5). As it can be seen, the most stable conformation is **b** and the energy differences among the structures are very small, where the less stable conformers **a** and **c** are only +0.7 and +0.3 kcal mol⁻¹, respectively, higher in energy than **b**. Thus, changing the conformation from **a** to **b** or **c** requires less than 1 kcal mol⁻¹. Moreover, the O–H bond distance in these structures is 0.970 Å, which may be used as a reference for the study of the fullerene system considered.

Thermodynamic calculations of the different conformers of the *N*-methylfulleropyrrolidine have shown that the most stable structures are **11(A)** and **11(B)** (see Figure 2). In the case of the most stable conformer **11(B)**, the substituent benzenediol has the most favorable conformation found for the model system **b** where one of the hydrogen atoms is forming a hydrogen bond (1.973 Å) with the nitrogen of the pyrrolidine ring. This theoretical prediction is in good agreement with the above ¹H

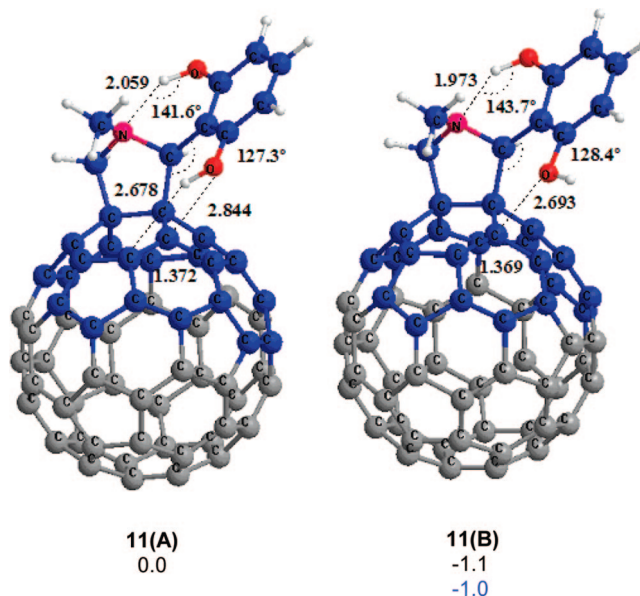


FIGURE 2. Optimized structures for **11(A)** and **11(B)** with the most relevant distances (Å) and angles (deg). The high level of the ONIOM approach is constituted by the colored atoms. The relative energy differences at the (ONIOM2(UB3LYP/6-31G(d):SVWN/STO-3G)) is represented by black, whereas blue is used for the single point calculation at (ONIOM2(MP2/6-31G(d):SVWN/STO-3G)//ONIOM2(UB3LYP/6-31G(d):SVWN/STO-3G)). All energies are expressed in kcal mol⁻¹.

NMR experimental findings. Because of that hydrogen bond, the bond distance (O–H) of the involved hydroxyl group has been increased up to 0.987 Å (in the model system it was 0.970 Å). The oxygen atom of the other hydroxyl group that is not interacting with the π -system of the fullerene surface has the same bond distance as in the model system, 0.970 Å.

The main difference between structures **11(A)** and **11(B)** is that the former has one of the hydrogen atoms of the hydroxyl groups interacting with the π -system of the fullerene surface. Those $\pi \cdots \text{H}$ interactions are relatively frequent in areas such as molecular clusters, molecular recognition, drug design, crystal packing, and so on. A large component of these $\pi \cdots \text{H}$ interactions comes from the London dispersion forces.³⁵ This long-range interaction (2.678 Å) does not have a remarkable stabilization effect, as product **11(B)** is 1.1 kcal mol⁻¹ more stable than **11(A)** at the ONIOM2(B3LYP/6-31G(d):SVWN/STO-3G) level of theory (this energy also includes the change on the O–H conformation, but we have seen in the model system that the energy difference associated with such conformational change is about +0.7 kcal/mol). However, it is well-known that current DFT methods do not, in general, properly describe dispersion interactions.³⁶ For instance, the sandwich configuration of benzene is not bound with the PW91, BLYP, and B3LYP exchange-correlation functionals.³⁷ Such interaction, however, is relatively well-described (somewhat overestimated) with the MP2 method.³⁸ For this reason, we have recomputed the energy differences at the ONIOM2(MP2/6-31G(d):SVWN/

(27) Slater, J. C. *Quantum Theory of Molecules and Solids*; McGraw-Hill: New York, 1974; Vol. 4.

(28) Vosko, S. H.; Wilk, L.; Nusair, M. *Can. J. Phys.* **1980**, *58*, 1200–1211.

(29) Hehre, W. J.; Stewart, R. F.; Pople, J. A. *J. Chem. Phys.* **1969**, *51*, 2657–2664.

(30) Becke, A. D. *J. Chem. Phys.* **1993**, *98*, 5648–5652.

(31) Lee, C.; Yang, W.; Parr, R. G. *Phys. Rev. B* **1988**, *37*, 785–789.

(32) Stephens, P. J.; Devlin, F. J.; Chabalowski, C. F.; Frisch, M. J. *J. Phys. Chem.* **1994**, *98*, 11623–11627.

(33) Hehre, W. J.; Ditchfield, R.; Pople, J. A. *J. Chem. Phys.* **1972**, *56*, 2257–2261.

(34) Hariharan, P. C.; Pople, J. A. *Theor. Chim. Acta* **1973**, *28*, 213–222.

(35) Spirko, V.; Hobza, P. *Chem. Phys. Chem.* **2006**, *7*, 640–643.

(36) (a) Van Mourik, T.; Gdanitz, R. *J. Chem. Phys.* **2002**, *116*, 9620–9623. (b) Ye, X.; Li, Z.-H.; Wang, W.; Fan, K.; Xu, W.; Hua, Z. *Chem. Phys. Lett.* **2004**, *397*, 56–61. (c) Godfrey-Kittle, A.; Caferio, M. *Int. J. Quantum Chem.* **2006**, *106*, 2035–2043. (d) Cerny, J.; Hobza, P. *Phys. Chem. Chem. Phys.* **2005**, *7*, 1624–1626. (e) Bautista-Ibáñez, L.; Ramírez-Gualito, K.; Quiroz-García, B.; Rojas-Aguilar, A.; Cuevas, G. *J. Org. Chem.* **2008**, *73*, 849–857.

(37) Tsuzuki, S.; Luthi, H. P. *J. Chem. Phys.* **2001**, *114*, 3949–3957.

STO-3G)//ONIOM2(B3LYP/6-31G(d):SVWN/STO-3G). Somewhat surprisingly, even at this level of theory **11(B)** is still more stable than **11(A)**, although now by only 1.0 kcal mol⁻¹. As expected in this kind of $\pi\cdots\text{H}$ interactions, the O–H bond distance of the hydroxyl group has been hardly modified (0.971 Å). It is worth mentioning that, quite often, this X–H distance becomes even shorter after the $\pi\cdots\text{H}$ interaction leading to the so-called blue-shift H-bonds.³⁹ This $\pi\cdots\text{H}$ interaction present in conformer **11(A)** leads to structural effects as the hydrogen bond between the other hydroxyl group and the nitrogen atom of the pyrrolidine ring becomes weaker (the H–N distance is 2.059 and 1.973 Å in conformers **11(A)** and **11(B)**, respectively). Therefore, the extra-stabilization of structure **11(B)** can be partially produced for the strongest hydrogen bond due to the lack of the above-mentioned $\pi\cdots\text{H}$ interaction.

Experimentally, it has been observed that the cycloaddition between compounds **1** and **7** leads to the fulleropyrrolidine derivatives **8** and **9**, where in the latter structure an insertion of the hydroxyl group of the benzene substituent is produced on the fullerene surface, leading to the cycled fullerene derivative **9**. It has also been found that the reaction is clearly favored when the carbon atom C-2 of the pyrrolidine ring is endowed with a methyl group instead of a hydrogen atom. To understand the origin of the effect of this methyl group on the whole process, we have studied by means of DFT calculations the mechanism of this O–H insertion to form the new compound **9** as well as the nonobtained compound **12** (similar to **9** but bearing a H atom instead of the methyl group on C-2 of the pyrrolidine ring). The calculated energy profile of the two reaction mechanisms are represented in Figure 3.

When the substituent on the carbon atom C-2 of the pyrrolidine ring is hydrogen, the reaction has a reaction energy of -9.6 kcal mol⁻¹, whereas in the case of the methyl substituent the reaction energy becomes slightly more favorable (-10.6 kcal mol⁻¹). The molecular structure of reactant **11** is shown in Figure 2 (species **11(A)**), and those of **8**, **9**, and **12** are depicted in Figure 4. We have optimized all possible conformers for species **9** and **12**, and those depicted in Figure 4 correspond to the most stable conformers. Although both systems present exothermic reaction energies, thermodynamic results favor the reaction when the methyl group is present.

From the two products **9** and **12** and by means of linear transit procedures, we have located the transition state structures **TS9** and **TS12** represented in Figure 5. We have found that the reaction is also favored from the kinetic point of view when the carbon C-2 of the pyrrolidine ring presents the -CH₃ group; the reaction barrier for the **8** → **9** process is relatively large (+40.6 kcal mol⁻¹) but still more favorable than in the **11** → **12** case (+43.0 kcal mol⁻¹). The Gibbs free energy of the reaction barriers obtained at 298 K are somewhat smaller at +39.7 and +37.5 kcal mol⁻¹ in the hydrogen and methyl case, respectively. The reaction is thermodynamically and kinetically more favorable for the methyl substituent case. The geometry optimization of each TS done by slightly shifting the geometry of the TS following the direction of the transition vector in the

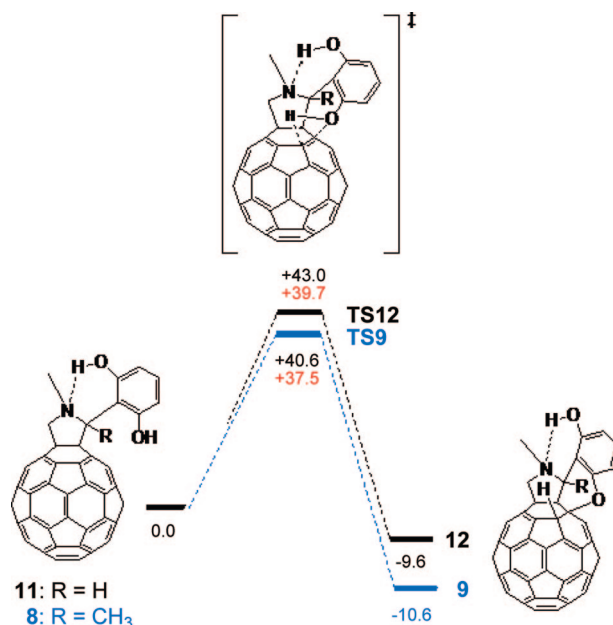


FIGURE 3. Representation of the reaction mechanisms profiles when the substituent R is a hydrogen (black) and a methyl group (blue). The energy values obtained with the ONIOM2(UB3LYP/6-31G(d):SVWN/STO-3G) method are expressed in kcal mol⁻¹. Red represents the free Gibbs energy barriers.

direction of the reactants indicated that **TS9** is connected with reactant **8** and **TS12** with reactant **11(A)**.

As it is shown in Figures 4 and 5, the introduction of the methyl substituent on the carbon C-2 of the pyrrolidine ring leads to important structural changes. Those structures with the above-mentioned substituent (**8**, **9**, and **TS9**) present a C–C–C angle involving the C-2 of the pyrrolidine ring as the central carbon of 113.8°, 115.5°, and 110.6° in the reactant (**8**), TS (**TS9**), and product (**9**) respectively, whereas this angle is 127.3°, 121.2°, and 114.6° for theoretical compounds **11**, **TS12**, and **12**, respectively. This variation on the angle induced by the absence/presence of the methyl substituent favors, in all cases, the interaction between the oxygen atom of the hydroxyl group and the [6,6] bond of the fullerene structure, because those atoms that will interact are located closer to the fullerene cage. The O–C distance of the new bond being formed during the insertion in reactants **11** and **8** is 2.844 and 2.725 Å, respectively. Moreover, the introduction of the methyl group favors the hydrogen bond formation between the other hydroxyl group of the benzene substituent and the nitrogen atom of the pyrrolidine ring. The H–N distance is modified from 2.059 Å in **11** to 2.654 Å in **12** for the hydrogen substituent case (there is a partial loss of this H-bond interaction along the OH insertion in this case), whereas when the methyl group is added this distance is approximately equal in either reactant, transition state, or final product (which is about 1.700 Å). Moreover, the N–H–O angle is modified upon the substituent change (141.6° and 147.5° in the case of **11** and **8**, respectively).

Therefore, theoretical calculations clearly support that the introduction of the methyl substituent on the carbon atom C-2 of the pyrrolidine ring leads to significant structural changes, which first reduce the distance between the oxygen and the carbon atom of the fullerene surface that will react, and second avoids partial loss of the favorable hydrogen bond interaction between the other hydroxyl group and the nitrogen atom of the pyrrolidine ring in the TS. These structural changes have

(38) (a) Sinnokrot, M. O.; Sherrill, C. D. *J. Phys. Chem. A* **2004**, *108*, 10200–10207. (b) Tsuzuki, S.; Honda, K.; Uchimaru, T.; Mikami, M.; Tanabe, K. *J. Am. Chem. Soc.* **2002**, *124*, 104–112. (c) Tsuzuki, S.; Uchimaru, T.; Matsumura, K.; Mikami, M.; Tanabe, K. *Chem. Phys. Lett.* **2000**, *319*, 547–554. (d) Lee, E. C.; Kim, D.; Jurecka, P.; Tarakeshwar, P.; Hobza, P.; Kim, K. S. *J. Phys. Chem. A* **2007**, *111*, 3446–3457.

(39) Hermida-Ramón, J. M.; Graña, A. M. *J. Comput. Chem.* **2006**, *28*, 540–546.

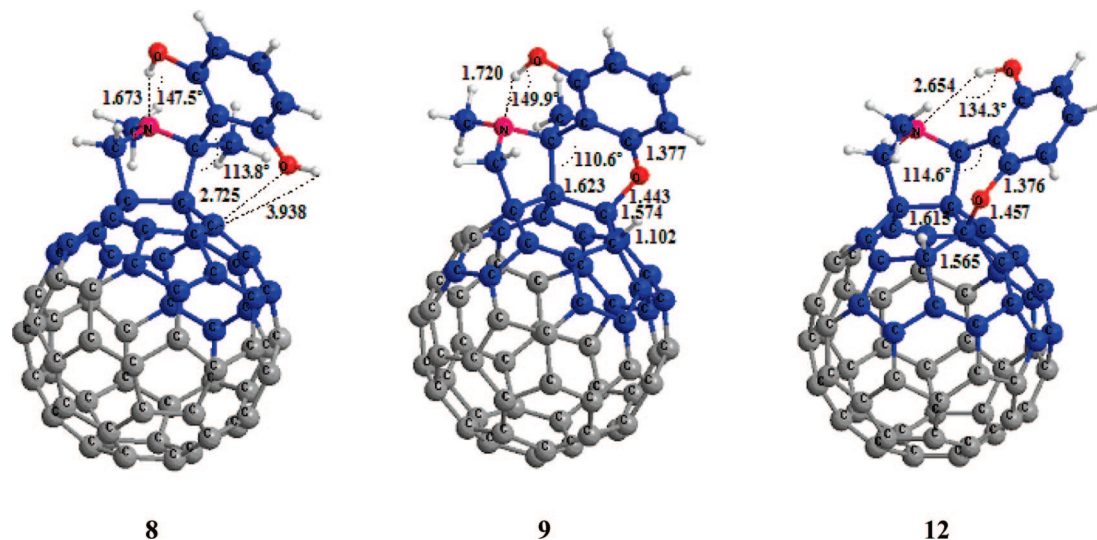


FIGURE 4. Optimized structure (ONIOM2(UB3LYP/6-31G(d):SVWN/STO-3G)) for **8**, **9**, and **12** with the most relevant distances (Å) and angles (deg). The high level of the ONIOM approach is constituted by the colored atoms.

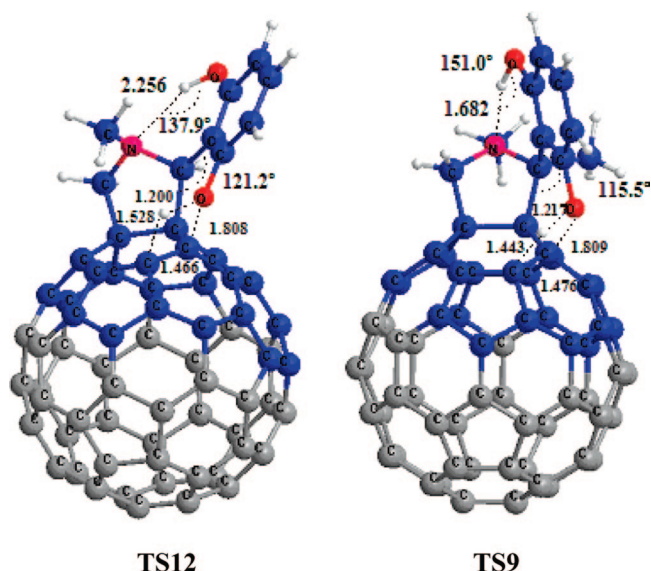


FIGURE 5. Optimized transition state structures (ONIOM2(UB3LYP/6-31G(d):SVWN/STO-3G)) for **TS12** and **TS9** with the most relevant distances (Å) and angles (deg). The high level of the ONIOM approach is constituted by the colored atoms.

thermodynamic and kinetic consequences, as the reaction is much more favored from both points of view, leading to a more exothermic reaction with a lower activation barrier.

Summary and Conclusions

In summary, we have studied for the first time the intramolecular nucleophilic addition of the hydroxyl group to the fullerene double bond adjacent to the pyrrolidine ring, in a totally regioselective process, affording the *cis-1* isomer. A crucial factor to accomplish the pyrano-fused fulleropyrrolidine **9** is the presence of a methyl group on C-2 of the pyrrolidine ring as a key requirement to optimize the approaching geometry of the OH group to the fullerene C=C and to help strengthen the H-bond interaction between the other hydroxyl substituent of the aryl group and the nitrogen atom of the pyrrolidine ring in the TS.

The existence of an intramolecular H-bond between the N atom of the pyrrolidine ring and a second OH group located on

the phenyl substituent on the C-2 atom of the pyrrolidine ring facilitates the geometrical approach of the OH group to the fullerene surface. However, the lack of cyclization from compound **11** bearing two hydroxyl groups reveals the presence of the methyl group on the pyrrolidine ring as the essential factor to form the cyclic compound.

Since the new compounds are readily available in a single synthetic step from 2,6-dihydroxyphenyl methyl ketones, this new reaction paves the way for the preparation of a variety of new heterocycle-fused fullerenes of interest in materials science as well as for testing their biological properties. Work is currently in progress to expand the reaction to alcohols and other heterocycles prepared from sulfur and nitrogen atoms as nucleophilic reagents.

Experimental Section

General Procedure for the Synthesis of Fulleropyrrolidines **3a, **3b**, **6**, and **11**.** To a solution of C₆₀ (0.25 mmol, 180 mg) in chlorobenzene (70 mL) were added 0.50 mmol of the carbonyl compound (salicylaldehyde for **3a**, 4,6-dimethoxysalicylaldehyde for **3b**, *o*-hydroxy phenylmethyl ketone for **6**, 2,6-dihydroxybenzaldehyde for **11**) and 0.50 mmol (for **3a**, **6**, and **11**) or 2.00 mmol of sarcosine (for **3b**). The mixture was refluxed overnight. After cooling, the solvent was removed in vacuo, and the crude product was purified by flash chromatography over silica gel, using initially CS₂ as eluent (to separate the unreacted fullerene) and then toluene/ethyl acetate 9:1 to obtain the corresponding product: **3a** in 13% yield (44% based on recovered C₆₀), **3b** in 33% yield (52% based on recovered C₆₀), **6** in 25% yield (50% based on recovered C₆₀), and **11** in 20% yield (28% based on recovered C₆₀).

Pyrrolidino[3,4:1,2][60]fullerene (3a**).** ¹H NMR (CDCl₃, 298 K, 300 MHz) δ 3.02 (s, 3H, CH₃), 4.31 (d, 1H, *J* = 9.7 Hz, CH₂-N), 5.11 (d, 1H, *J* = 9.7 Hz, CH₂-N), 5.14 (s, 1H, CH-N), 6.90 (dd, 2H, *J* = 8.08, 7.6 Hz, H-Ar), 7.24 (d, 1H, *J* = 7.6 Hz, H-Ar), 7.39 (d, 1H, *J* = 7.6 Hz, H-Ar), 11.12 (s, 1H, OH); ¹³C NMR (CDCl₃, 298 K, 75 MHz) δ 41.0, 69.1, 70.0, 77.6, 84.2, 110.7, 117.9, 119.9, 120.0, 128.1, 130.3, 130.7, 130.9, 135.7, 136.0, 137.1, 137.4, 139.7, 140.4, 140.5, 140.6, 141.9, 142.0, 142.1, 142.3, 142.4, 142.48, 142.50, 142.53, 142.56, 142.6, 142.9, 142.99, 143.0, 143.1, 143.4, 143.5, 144.7, 144.8, 145.0, 145.03, 145.5, 145.6, 145.69, 145.7, 145.8, 145.9, 145.99, 146.0, 146.2, 146.3, 146.4, 146.5, 146.6, 146.65, 146.7, 146.8, 146.83, 147.7, 147.8, 151.5, 152.0, 153.3, 153.6, 155.5, 157.2, 162.1; FTIR (KBr, cm⁻¹) 526.28, 574.32, 1184.71, 1432.18; MS (MALDI TOF) *m/z* 869 [M⁺].

Pyrrolidino[3,4:1,2][60]fullerene (3b). ¹H NMR (CDCl₃/CS₂, 298 K, 500 MHz) δ 2.98 (s, 3H, CH₃-N), 3.68 (s, 3H, OCH₃), 3.76 (s, 3H, OCH₃), 4.30 (d, 1H, *J* = 9.6 Hz, CH₂-N), 5.07 (d, 1H, *J* = 9.6 Hz, CH₂-N), 5.70 (s, 1H, CH-N), 5.99 (d, 1H, *J* = 2.3 Hz, H-Ar), 6.04 (d, 1H, *J* = 2.3 Hz, H-Ar), 11.59 (s, 1H, OH); ¹³C NMR (CDCl₃/CS₂, 298 K, 125 MHz) δ 41.0, 55.5, 55.7, 69.2, 69.8, 76.8, 91.4, 94.8, 101.7, 128.7, 134.6, 136.2, 136.7, 137.3, 138.2, 138.4, 139.2, 139.9, 140.0, 140.6, 140.7, 142.0, 142.1, 142.12, 142.4, 142.5, 142.59, 142.6, 142.66, 142.7, 143.0, 143.09, 143.1, 143.4, 144.79, 144.8, 144.9, 145.1, 145.5, 145.57, 145.6, 145.65, 145.7, 145.8, 145.9, 146.0, 146.2, 146.3, 146.4, 146.5, 146.57, 146.6, 146.67, 146.7, 146.74, 146.8, 147.1, 147.7, 147.8, 153.2, 153.4, 155.1, 156.1, 159.6, 159.65, 162.1; MS (ESI) *m/z* 929 [M⁺]

Pyrrolidino[3,4:1,2][60]fullerene (6). ¹H NMR (CDCl₃, 298 K, 300 MHz) δ 2.45 (s, 3H, CH₃), 2.97 (s, 3H, CH₃-N), 4.74 (d, 1H, *J* = 10.1 Hz, CH₂-N), 4.97 (d, 1H, *J* = 10.1 Hz, CH₂-N), 6.90–6.85 (m, 2H, H-Ar), 7.20 (bs, 1H, H-Ar), 7.52 (dd, 1H, *J* = 8.2, 1.5 Hz, H-Ar), 13.13 (s, 1H, OH); ¹³C NMR (CDCl₃, 298 K, 75 MHz) δ 18.1, 35.4, 65.0, 68.0, 79.1, 80.9, 118.3, 119.8, 125.0, 128.1, 128.5, 130.6, 130.9, 132.96, 136.4, 136.5, 136.7, 136.9, 139.3, 140.2, 140.5, 140.6, 141.6, 141.8, 141.9, 142.0, 142.4, 142.5, 142.57, 142.6, 142.7, 142.8, 143.0, 143.1, 143.5, 144.8, 145.0, 145.07, 145.5, 145.6, 145.69, 145.7, 145.74, 145.8, 146.0, 146.2, 146.27, 146.3, 146.4, 146.5, 146.57, 146.6, 146.68, 146.7, 146.8, 146.9, 147.8, 153.0, 153.3, 153.9, 156.2, 158.5; FTIR (KBr, cm⁻¹) 526.58, 575.56, 1155.64, 1462.13; MS (MALDI TOF) 883 [M⁺].

Pyrrolidino[3,4:1,2][60]fullerene (11). ¹H NMR (CDCl₃, 298 K, 300 MHz) δ 2.99 (s, 3H, CH₃), 4.35 (d, 1H, *J* = 9.9 Hz, CH₂-N), 5.02 (s, 1H, OH), 5.09 (d, 1H, *J* = 9.9 Hz, CH₂-N), 5.81 (s, 1H, CH-N), 6.32 (d, 1H, *J* = 8.1 Hz, H-Ar), 6.51 (d, 1H, *J* = 8.1 Hz, H-Ar), 7.07 (t, 1H, *J* = 8.1 Hz, H-Ar), 11.77 (s, 1H, OH); ¹³C NMR (CDCl₃, 298 K, 75 MHz) δ 39.6, 67.9, 68.3, 68.6, 75.3, 105.4, 106.5, 109.5, 127.5, 128.5, 129.4, 133.7, 134.8, 135.4, 135.8, 136.0, 138.6, 138.7, 139.2, 139.3, 140.6, 140.66, 140.7, 140.8, 141.0, 141.1, 141.15, 141.18, 141.2, 141.3, 141.4, 141.6, 141.7, 141.75, 142.0, 142.1, 143.3, 143.4, 143.5, 143.6, 143.7, 144.1, 144.2, 144.25, 144.3, 144.33, 144.4, 144.5, 144.7, 144.8, 144.9, 145.0, 145.08, 145.1, 145.2, 145.25, 145.28, 145.3, 145.4, 145.7, 145.8, 146.3, 146.4, 151.4, 152.0, 153.6, 154.3, 154.4, 157.9; FTIR (KBr, cm⁻¹) 529.08, 1182.63, 1460.64.

Synthesis of Pyrrolidino[3,4:1,2][60]fullerenes 8 and 9. To a solution of 0.50 mmol (360 mg) of C₆₀ in chlorobenzene (80 mL) were added 0.75 mmol (114 mg) of 2,6-dihydroxyphenyl methyl ketone (7) and 2.0 mmol (178 mg) of sarcosine. The mixture was refluxed overnight, and after cooling to room temperature, the solvent was removed in vacuo. The crude product was purified by flash chromatography over silica gel, using toluene/ethyl acetate 9:1 to obtain compound 8 in 12% yield and compound 9 in 31% yield.

Compound 8 was further converted quantitatively to 9 by refluxing in chlorobenzene for 4 h.

Compound 8. ¹H NMR (CDCl₃, 298 K, 300 MHz) δ 2.75 (s, 3H, CH₃), 3.00 (s, 3H, CH₃-N), 4.72 (AB system, 2H, CH₂N), 4.75 (s, 1H, OH), 6.16 (dd, 1H, *J* = 8.0, 1.1 Hz, H-Ar), 6.45 (dd, 1H, *J* = 8.0, 1.1 Hz, H-Ar), 6.99 (t, 1H, *J* = 8.0 Hz, H-Ar), 13.92 (s, 1H, OH); ¹³C NMR (CDCl₃/CS₂, 298 K, 75 MHz) δ 30.4, 35.6, 63.9, 68.0, 80.1, 80.7, 108.0, 111.7, 112.8, 128.7, 130.4, 135.6, 136.5, 137.2, 139.1, 139.7, 140.6, 140.7, 141.9, 142.0, 142.07, 142.1, 142.2, 142.4, 142.47, 142.5, 142.7, 142.77, 142.8, 142.81, 143.0, 143.08, 143.1, 143.4, 143.5, 143.6, 144.8, 145.0, 145.1, 145.4, 145.5, 145.6, 145.7, 145.76, 145.8, 145.9, 146.1, 146.2, 146.3, 146.4, 146.5, 146.56, 146.6, 146.62, 146.7, 146.8, 146.83, 147.8, 147.9, 148.1, 153.7, 154.3, 154.4, 155.8, 156.3, 160.9; FTIR (KBr, cm⁻¹) 526.50, 574.57, 1151.88, 1452.16; MS (ESI) *m/z* 898 [M⁺].

Compound 9. ¹H NMR (CDCl₃, 298 K, 300 MHz) δ 2.18 (s, 3H, CH₃), 3.54 (s, 3H, CH₃), 4.76 (d, 1H, *J* = 12.7 Hz, CH₂N), 5.00 (d, 1H, *J* = 12.7 Hz, CH₂-N), 6.29 (s, 1H, H-C₆₀), 6.85 (dd, 1H, *J* = 7.9, 1.1 Hz, H-Ar), 7.03 (dd, 1H, *J* = 7.9, 1.1 Hz, H-Ar), 7.39 (t, 1H, *J* = 8.0 Hz, H-Ar), 13.23 (s, 1H, OH); ¹³C NMR (CDCl₃/CS₂, 298 K, 75 MHz) δ 36.5, 57.3, 66.2, 71.3, 75.4, 79.4, 92.4, 111.2, 113.7, 117.7, 130.0, 134.4, 135.5, 135.7, 136.2, 137.6, 140.8, 140.9, 141.6, 142.3, 142.46, 142.5, 142.6, 142.7, 142.8, 143.0, 143.2, 143.4, 143.6, 143.8, 143.9, 144.0, 144.04, 144.2, 144.3, 144.4, 144.5, 144.6, 144.7, 144.9, 145.1, 145.2, 145.3, 145.9, 146.1, 146.3, 146.5, 146.6, 146.9, 147.0, 147.05, 147.3, 147.9, 148.2, 148.7, 149.0, 149.1, 149.2, 150.1, 152.8, 154.0, 157.9; FTIR (KBr, cm⁻¹) 526.90, 575.17, 1197.22, 1462.20; MS (ESI) *m/z* 898 [M⁺].

Acknowledgment. This work was supported by the MEC of Spain (project CT2005-02609/BQU, project CTQ2008-03077/BQU and Consolider-Ingenio 2010C-07-25200), the CAM (project P-PPQ-000225-0505) and the Catalan Departament d'Universitats, Recerca i Societat de la Informació (DURSI) of the Generalitat de Catalunya project 2005SGR-00238. S.F. thanks the MEC for a Ramón y Cajal contract, and S.O. thanks the MEC for Doctoral Fellowship AP2005-2992. M.I. thanks the European Science Foundation for Predoctoral contract (SOHYD 05-SONS-FP-021).

Supporting Information Available: General procedure for the synthesis of fulleropyrrolidines 3a, 3b, 6, and 11. ¹H NMR, ¹³C NMR, and MS spectra of all compounds. HPLC of compounds 8 and 9. CV voltammogram of compound 6 and table of reduction potentials. Xyz optimized Cartesian coordinates and total energies for all minima and transition states located. Optimized structures and relative energies for the different conformers of species 3a and 6. This material is available free of charge via the Internet at <http://pubs.acs.org>.

JO802152X